

# Exploring of a potential energy surface around a valley bifurcation

Wolfgang Quapp<sup>1\*</sup>, Grace Hsiao-Han Chuang<sup>2</sup> and Josep Maria Bofill<sup>3,4</sup>

<sup>1\*</sup>Mathematisches Institut, Universität Leipzig, Augustus-Platz PF 100920, Leipzig, D-04009, Germany, Orcid: 0000-0002-0366-1408.

<sup>2</sup>Physics of Complex Systems, Max Planck Institute, Noethnitzer Str. 38, Dresden, D-01187, Germany, Orcid: 0000-0003-0145-9596.

<sup>3</sup>Química Inorgànica i Orgànica, Secció de Química Orgànica, Universitat de Barcelona, Martí i Franquès 1, Barcelona, 08028, Catalunya, Spain, Orcid: 0000-0002-0974-4618.

<sup>4</sup>Institut de Química Teòrica i Computacional (IQTUB), Universitat de Barcelona, Martí i Franquès 1, Barcelona, 08028, Catalunya, Spain.

\*Corresponding author(s). E-mail(s): [quapp@math.uni-leipzig.de](mailto:quapp@math.uni-leipzig.de);  
Contributing authors: [hhchuang@pks.mpg.de](mailto:hhchuang@pks.mpg.de); [jmbofill@ub.edu](mailto:jmbofill@ub.edu);

## Abstract

**Purpose:** Valley-ridge inflection (VRI) points play an important role in organic chemistry, especially in post-TS bifurcations. We explain a new discovery of a special structure of the region with another, weaker type of a valley bifurcation (VB) without a ridge in between.

**Methods:** We apply the theory of Newton trajectories (NTs) and gradient extremals (GEs) to cases of two dimensional potential energy surfaces.

**Results:** We define an indicator of the valley bifurcation where the gradient of the potential energy surface is the eigenvector of the Hessian matrix at eigenvalue zero.

**Conclusion:** The new type of bifurcation point is connected with a ‘dead’ valley of the PES. The example is a nice demonstration that the index theorem for NTs holds, nevertheless. NTs and GEs are important tools to explore the region of the bifurcation point.

25-3-2025      Revision 29-5-2025

**Keywords:** Potential energy surface, Transition state, Valley-ridge inflection point, Valley bifurcation, Regular and singular Newton trajectory, Gradient extremal

# 047 1 Introduction

048  
049 Bifurcations are omnipresent in natural sciences [1, 2], including valleys on a poten-  
050 tial energy surface (PES). They are a long studied subject [3–8]. The bifurcation can  
051 take place before the transition state (TS) of a dissociation [9, 10], as it is demon-  
052 strated by an internal vibrational redistribution [11]. It also can happen at the TS  
053 [12, 13]. Or in contrast, the study of organic chemical reactions shows often bifurca-  
054 tions after the first TS. The theoretical understanding of the underlying mechanisms  
055 that govern selectivity, i.e. product distributions is of central interest [14–19]. And  
056 finally, the bifurcation can coalesce with a TS [6, 20]. Bifurcations can also take place  
057 in radiationless deactivation of organic dyes on the lower PES [21].

058 Understanding in particular asymmetric post-transition state bifurcations is essen-  
059 tial for predicting reaction selectivity in complex chemical systems [22, 23]. Of course,  
060 here the reaction pathways inherently require at least a two-dimensional (2D) descrip-  
061 tion, as long as a pathway over a single transition state bifurcates into two distinct  
062 product pathways. The PES has two consecutive saddles of index 1 with no interven-  
063 ing energy minimum. Between the two index-1 saddles, one of which has higher energy  
064 than the other, there must be a valley ridge inflection (VRI) point [6, 24–28].

065 The reaction is initiated when a trajectory crosses the area of the higher saddle  
066 (forming the entrance channel) and may approach the lower energy saddle. On either  
067 side of the lower energy saddle, there are two minimum wells. The question of interest  
068 is which well does the trajectory enter (predicting the product selectivity)? It could  
069 leave the standard intrinsic reaction path, the IRC [29–32].

070 One can assume that the VRI plays a role in selectivity. Certainly the VRI is a  
071 geometrical feature of the PES. Two conditions are fulfilled there: The curvature of  
072 the PES is zero, which implies that the Hessian matrix has a zero eigenvalue, and the  
073 gradient of the potential is perpendicular to the eigenvector corresponding to the zero  
074 eigenvalue. This means that the landscape of the PES in the neighborhood of the VRI  
075 changes its shape from a valley to a ridge which gave the region the name VRI.

076 In synthetic chemistry, identifying the key functional groups that influence reaction  
077 pathways is crucial for designing efficient synthesis strategies, especially when dealing  
078 with large molecules containing multiple functional groups. If the dominant degrees  
079 of freedom are known, especially the VRI region, chemists can target these features  
080 to streamline synthesis.

081 In this paper we analyse cases where a valley bifurcation occurs without an inter-  
082 vening ridge. We call this event valley bifurcation (VB). In the next Section we repeat  
083 the definition of the reaction path models of interest: Newton trajectories (NTs) and  
084 gradient extremals (GEs). In Section III we discuss different relations of a VRI region  
085 to the singular NT traversing it, and of cases of onyl VB, for different 2D test PES.  
086 In Section VI we add a discussion. A conclusion is given in Section V. Appendix 1-  
087 3 reports on the index theorem of NTs, the avoided crossing of GEs, and the 2D  
088 representation of NTs or GEs.

089  
090  
091  
092

## 2 Models of the reaction path

### 2.1 Newton trajectory

This work concerns a mathematical excursion which discusses the use of NTs for the exploration of a special PES,  $V(\mathbf{x})$  given in reference [33], and in particular its VRI or VB points. An NT is a curve  $\mathbf{x}(t)$  where the gradient,  $\mathbf{g}$ , of the PES is parallel to a given direction,  $\mathbf{f}$ , at every point

$$\mathbf{g}(\mathbf{x}(t)) \parallel \mathbf{f}, \quad (1)$$

$t$  is a curve length parameter. Curves that solve Eq.(1) are of particular interest in mechanochemistry, where the direction  $\mathbf{f}$  is the direction of an external force [34–36]. A possibility to follow a curve fulfilling this property (1) is the definition of a projector matrix. If  $\mathbf{r} = \mathbf{f}/|\mathbf{f}|$  is the normalized direction then

$$\mathbf{P} = (\mathbf{I} - \mathbf{r}\mathbf{r}^T)$$

projects on direction  $\mathbf{r}$ . Eq.(1) looks then

$$\mathbf{P} \mathbf{g}(\mathbf{x}(t)) = \mathbf{0}.$$

Its derivation can be used to develop a predictor-corrector method [6].

Alternatively, the approach of Eq.(1) was formulated in a differential equation by Branin [6, 37, 38]

$$\frac{d\mathbf{x}(t)}{dt} = \pm \text{Det}(\mathbf{H}(\mathbf{x}(t))) \mathbf{H}^{-1}(\mathbf{x}(t)) \mathbf{g}(\mathbf{x}(t)), \quad (2)$$

$\mathbf{H}$  is the Hessian of the second derivatives of the PES. It is important that the matrix

$$\mathbf{A} = \text{Det}(\mathbf{H}) \mathbf{H}^{-1} \quad (3)$$

is desingularized when the Hessian becomes singular. It is called the adjoint matrix for  $\mathbf{H}$ . The full Hessian matrix can be computationally expensive at each step of the positions  $\mathbf{x}(t)$ . However, it can be updated [39–41]. A first numerical step starts from a stationary point in direction  $\mathbf{f}$ . The following steps then ensure that the gradient maintains this direction [6]. The plus + sign in Eq.(2) is used for an NT from a minimum to an SP of index one, but the minus - vice versa. If the energy increases monotonically along an NT then it can serve for a reaction path variable.

Note that NTs have the nice property that they connect stationary points with an index difference of one [6, 38, 42], compare appendix 1. The index here counts the number of negative eigenvalues of the Hessian matrix at the stationary point. If we start at a minimum with index zero, we obtain a next saddle point (SP) with index one. A special case is a singular NT that crosses a valley ridge inflection (VRI) point [6]. The characterization of the VRI is the zero point of the right hand side of the

139 Branin equation (2)

$$140 \quad \mathbf{A} \mathbf{g} = \mathbf{0} \quad (4)$$

141 but where the gradient is not zero,  $\mathbf{g}(\mathbf{x}) \neq \mathbf{0}$ . We call it VRI point. A singular NT has  
142 four branches through the VRI point. It typically connects a minimum with a saddle  
143 of index two and two SPs of index one via the VRI. A VRI represents the branching of  
144 a valley into two valleys and an intermediate ridge, or complementarily, the branching  
145 of a ridge into two ridges and a valley in between. Mathematically, the Hessian has a  
146 zero eigenvector orthogonal to the gradient [6, 8, 31, 43, 44].

147 We can follow a one-dimensional curve by Eq. (2) in any dimension. For a PES  
148 with more than two dimensions manifolds of VRI points arise [45, 46]. There is an  
149 illustrative introduction to the higher dimensional case [47]. The following of an NT  
150 is included in the COLUMBUS program system [48] (under the name reduced gradi-  
151 ent following, RGF). There are some links to different programs [49, 50]. If the PES is  
152 symmetric, the VRI manifold often forms a symmetry hypersurface. However, asym-  
153 metric VRI manifolds can also be computed [45, 49, 51, 52]. Recently, the role of VRI  
154 points in dynamical processes has been discussed [53]. The Newton trajectory method  
155 has been established in chemistry since 1998, see refs. [36, 54–59] and further refer-  
156 ences therein. We report that NTs are calculated for medium molecules with up to  
157 dimension 486 [60].

## 159 2.2 Gradient extremal

160  
161 A second kind of curves which also can serve for the description of reaction valleys are  
162 gradient extremals (GE) [6, 61–64] where holds

$$164 \quad \mathbf{H}(\mathbf{x}(t))\mathbf{g}(\mathbf{x}(t)) = \lambda \mathbf{g}(\mathbf{x}(t)) \quad (5)$$

165  
166 thus on a GE the gradient,  $\mathbf{g}$ , is an eigenvector of the Hessian,  $\mathbf{H}$ , with (varying)  
167 eigenvalue  $\lambda$ . GEs are represented in the following figures by black dashed curves. A  
168 VRI point is crossed by a GE if the pseudo-convexity index  $\mu$  [65, 66] changes its sign

$$170 \quad \mu = \frac{\mathbf{g}^T \mathbf{A} \mathbf{g}}{\mathbf{g}^T \mathbf{g}} . \quad (6)$$

171  
172  
173 Below we explain a new type of a valley bifurcation (VB) region by the crossing of  
174 a GE with an index boundary line, Eq. (7). Then the condition (6) does not apply.

175 GEs can bifurcate itself [62, 63, 67]. This happens when the two eigenvalues,  $\lambda$  in  
176 Eq. (5), of the two intersecting branches become equal. Normally, however, these two  
177 equal eigenvalues are not zero. Therefore, no VRI point is indicated by such a crossing.  
178 But the GE crossing can indicate the change of a valley ground into a circe [67]. Then  
179 the bifurcation of the GE can be an indication on a nearby VB or VRI event. A pitch  
180 fork GE is, in a sense, a preview to a VB or a VRI point. On an asymmetric PES,  
181 however, the normal case is the avoided crossing of the GEs. We report an example  
182 in appendix 2.

183  
184

Typically,  $N$  GEs emanate from a stationary point, if  $N$  is the dimension of the PES. Then the GE to the smallest eigenvalue  $\lambda_{min}$  describes the baseline of the reaction valley. This GE can be considered a static representation of a reaction path.

### 2.3 Index boundary

Another interesting type of curves is the boundary between regions of a different index of the Hessian of the PES. For the case of 2D surfaces  $V(x, y)$  they are given by

$$Det(\mathbf{H}) = V_{xx} V_{yy} - V_{xy}^2 = 0 \quad (7)$$

and these index boundaries (IB) are represented by thin green curves in the following figures.

## 3 2D example PES

A series of PES is used of Ref.[33]

$$V(x, y) = x^4 - 2x^2 + y^4 + y^2 - 1.5x^2y^2 + x^2y - cy^3 \quad (8)$$

as shown in the following figures. The constant  $c$  is a parameter that varies here between 1 and 2.

### 3.1 PES for $c=1.5$

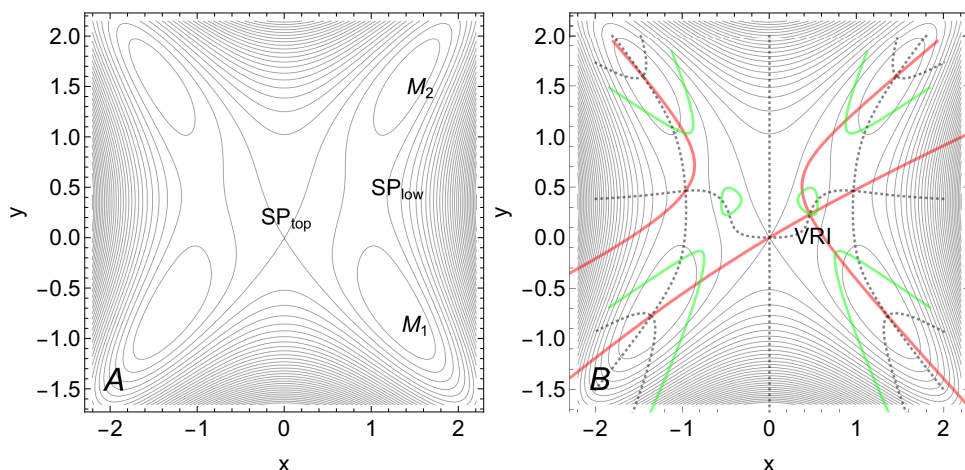


**Fig. 1** **A:** Level lines of PES (8) for  $c=1.5$ . The axis  $x=0$  is an axis of symmetry.  $M_1$  is a minimum,  $SP_{low}$  is the transition state to the minimum  $M_2$ . The global  $SP_{top}$  lies central on the  $y$  axis at point  $(0, 0)$ . **B:** A VRI point is located between  $SP_{top}$  and the stationary points in the valley on the right hand side. Three types of curves are shown: Bold red is the singular NT through the right VRI point, GE curves are dashed black, and the IB-lines are thin green.

231  
232  
233  
234  
235  
236  
237  
238  
239  
240  
241  
242  
243  
244  
245  
246  
247  
248  
249  
250  
251  
252  
253  
254  
255  
256  
257  
258  
259  
260  
261  
262  
263  
264  
265  
266  
267  
268  
269  
270  
271  
272  
273  
274  
275  
276

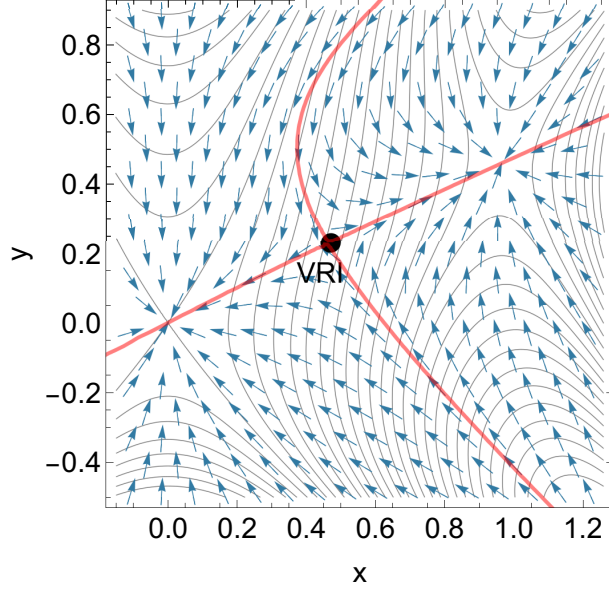


**Fig. 2** Vector field of the Branin Eq.(2) with plus sign on a section of the PES of Fig. 1. The VRI point is characterized by the hyperbolic touching of the corresponding regular NTs.

First we discuss a ‘normal’ case for parameter  $c=1.5$  of PES (8). One can observe in Fig.1 that the right valley from  $M_1$  to  $M_2$  bifurcates to the  $SP_{top}$ . There are only stationary points of index zero, minima, and of index one, transition states (TS). By different curves we can determine the exact VRI point. This is demonstrated in Fig.1B. Here the 4 branches of the singular red NT intersect at the VRI. The search direction of the singular NT is  $\mathbf{f}_{red}=(-1.3, 0.33)$ . It is the gradient at the solution of Eq.(4). The VRI is at  $(x, y)=(0.47, 0.23)$  with

$$\mathbf{g} = \begin{pmatrix} -1.32 \\ 0.34 \end{pmatrix}, \quad \mathbf{H} = \begin{pmatrix} -1.13 & 0.29 \\ 0.29 & -0.07 \end{pmatrix} \quad \text{and} \quad \mathbf{A} = \begin{pmatrix} -0.07 & -0.29 \\ -0.29 & -1.13 \end{pmatrix}.$$

The vector with Eq.(4) is  $\mathbf{A} \mathbf{g} = \mathbf{0}$  thus the gradient is the zero eigenvector of  $\mathbf{A}$ , and the second eigenvalue is  $\lambda = -1.204$  being the eigenvalue of the matrix  $\mathbf{H}$  for the eigenvector  $\mathbf{g}$ . The vector

$$\mathbf{v} = \begin{pmatrix} 0.34 \\ 1.32 \end{pmatrix}$$

is then the zero eigenvector of the Hessian orthogonally to the gradient. It is the characteristic of the VRI point. Note that Hessian and adjoint Hessian have the same eigenvectors, but for the eigenvalues  $\lambda_i$  of the Hessian and  $\mu_i$  of the adjoint the following applies for every  $i$  [68, 69]

$$\mu_i \lambda_i = \text{Det}(\mathbf{H}) = \prod_{k=1}^N \lambda_k. \quad (9)$$

For  $N = 2$  it means  $\mu_1 = \lambda_2$ ,  $\mu_2 = \lambda_1$ .

A thin green border line of  $\text{Det}(\mathbf{H})$  crosses a GE there. Thus, all three curves cross at the VRI point. (The calculation of these curves is described in appendix 3.) The boundaries of the different  $\text{Det}(\mathbf{H})$  regions are given by the condition of Eq.(7). Normally they are curvilinear, so that the points of a molecule on a higher dimensional PES with the IB condition  $\text{Det}(\mathbf{H}) = \mathbf{0}$  form curved hypersurfaces.

The VRI is intersected by its own singular NT which is represented by the bold red lines. The four branches form an almost orthogonal cross at the VRI point. This is the long known type of a valley bifurcation. Singular NTs are the boundaries of families of NTs that connect the minimums,  $M_i$ , to different  $SPs$ . Any two neighboring branches of the singular NT form a corridor for all NTs connecting a given minimum,  $M$ , with the same  $SP_i$  [70]. The stationary points are also crossed by the NT and by the various branches of the GEs.

In Fig.2, the vector field of the right hand side of the Branin Eq.(2) is included on the PES with  $c=1.5$ . The hyperbolic touching of the corresponding NTs before and after the VRI point is a characterization of this region.

### 3.2 PES for $c=1$

A 3D representation of this PES is shown in Fig.3. Here we develop the case of interest for a VB with a nonsingular NT, because a singular NT is missing, but a GE is included again. One can observe in Fig.4 that the right valley from  $M_1=M$  uphill

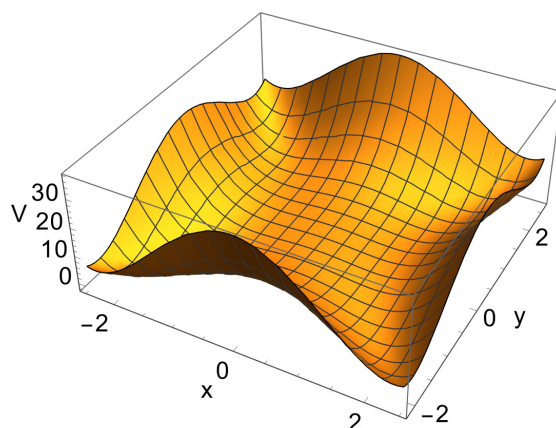


**Fig. 3** 3D representation of PES (8) for  $c=1$ . Only two uphill valleys remain. There are still two minima at the bottom, and the central SP also remains.

to the right hand side bifurcates again to a valley to the  $SP_{top} = SP$ , the only SP which remains. There is also a thin green border line, as well as a GE which crosses it. The gradient is the eigenvector of the Hessian, this is the general definition along the GE curves. Here for an intersection with the IB line the corresponding eigenvalue is zero. We take this crossing as the indicator for the VB point of a new type. It shows additionally the property that the zero eigenvector, the gradient, is nearly orthogonal

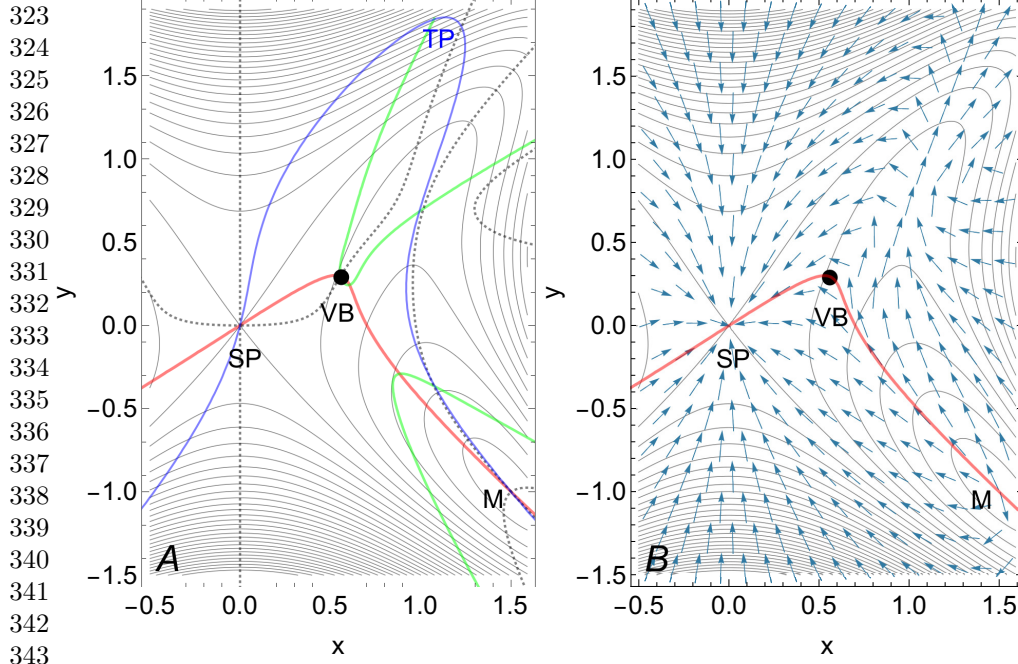


**Fig. 4** **A:** Three kinds of curves are drawn on the PES for  $c=1$ . Red is the remainder of the former singular NT through the VB point, black dashed are the GE curves, and green are the IB-lines. The blue curve is an ordinary regular NT. **B:** Vector field of Branin Eq.(2). The VB point is embedded in a nice flow of regular NTs.

to the direction of the GE. So the GE touches a level line. The first condition is

$$\mathbf{H} \mathbf{g} = \mathbf{0} . \quad (10)$$

It is in contrast to a VRI point where the zero eigenvector is orthogonal to the gradient, Eq. (4). We find a fairly regular NT connection the SP with the minimum M over this VB point. It is at  $(x,y)=(0.56,0.3)$  with

$$\mathbf{g} = \begin{pmatrix} -1.35 \\ 0.47 \end{pmatrix}, \quad \mathbf{H} = \begin{pmatrix} 0.04 & 0.13 \\ 0.13 & 0.35 \end{pmatrix} \quad \text{and} \quad \mathbf{A} = \begin{pmatrix} 0.35 & -0.13 \\ -0.13 & 0.04 \end{pmatrix}.$$

The search direction of the nonsingular NT is  $\mathbf{g}=\mathbf{f}_{red}=(-1.3533,0.468)$ . The Hessian matrix has the zero eigenvector being the gradient, and

$$\mathbf{A} \mathbf{g} = \begin{pmatrix} -0.53 \\ 0.18 \end{pmatrix} = 0.39 \mathbf{g} \neq \begin{pmatrix} 0 \\ 0 \end{pmatrix} .$$

A zero eigenvector of the Hessian is retained by the gradient, in this case. But 0.39 is the second eigenvalue of the direction orthogonal to the gradient. The value of the Branin vector is not zero which really shows that there is no 'normal' VRI point from the point of view of NTs. This is also an indication that such cases cannot be determined by the VRI finding method using the condition  $\mathbf{A} \mathbf{g}=\mathbf{0}$  [51, 52]. Additionally,



also  $\mu$  of definition (6) does not change its sign, thus it does not indicate the VRI point. Nevertheless the GE crosses the IB-line and has there the special eigenvalue  $\lambda = 0$ . We name this VB point for its crossing only by a GE. No bifurcation of a reaction trajectory takes place here. The condition  $\mathbf{H}\mathbf{g} = \mathbf{0}$ , at the other hand, is the criterion for an optimal barrier breakdown point (oBBP) in mechanochemistry [34–36]. But that is another story. The neighboring GE going uphill in the right valley ground intersects two times an IB line. However, the gradient there points in direction of the GE, not orthogonal to it. For the given VB point it is more appropriate to use the GE being between the two bifurcating valleys.

With the blue NT in Fig.4 A we add a regular NT beginning at minimum M and initially following the valley uphill. It shows a turning point (TP) high in the PES mountains where the energy reaches a maximum, and it returns as a regular connection to the only remaining SP at point (0, 0). Its search direction is  $\mathbf{f}_{blue} = (-0.53, 1.11)$ . The blue NT is an indication of the reason why this special VB point is useless for chemistry: The valley at the right hand side is a ‘dead’ valley without a further TS and minimum. There cannot be a stable chemical structure. On the right side of the PES only one minimum and one SP exist. Every NT starting in the right minimum has to find its way to the central SP. There are no other stationary points, so the NT through the VB point must also be ‘regular’. There is no target for it to bifurcate to. The entire right half-plane is one reaction channel [70]. The VB point exists but the index theorem acts that the VB does not disturb the channel of regular NTs. Note that the NT through the VB crosses nearby the IB-line a second time in the vicinity. We do not select the special NT with a single, tangential touch of the IB line for the definition of this new type of VB points.

In Fig.4 B the vector field of the right hand side of the Branin Eq.(2) is again included. The NTs flow around the VB point. Their hyperbolic contact at the VB point is lost.

### 3.3 Action of the index theorem for singular NTs

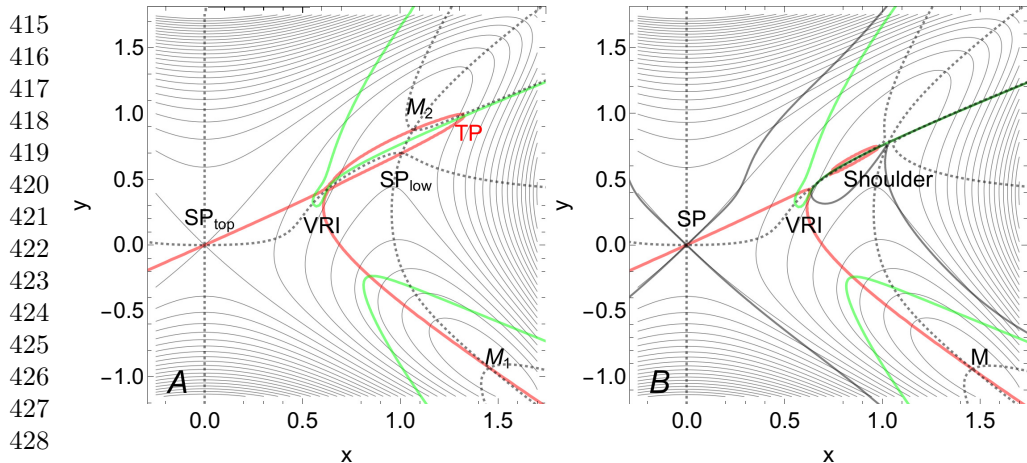
#### Index Theorem for NTs

Regular NTs connect stationary points with an index difference of one [6, 38, 42]. This will be violated by a singular NT.

**Proof:** see appendix 1.

Fig.5 A represents a quasi shoulder region of the former  $SP_{low}$  and the former minimum  $M_2$  for parameter  $c = 1.125$ . The two branches of the singular NT to  $SP_{low}$  and to the minimum  $M_2$  come close together. They form quasi parallel branches. After the two stationary points they continue and end in a TP. The four branches intersect at a small angle at the VRI point. However, the index theorem also applies here in its usual form. Stationary points are connected by regular NTs (not shown) and the singular NT connects with two branches the two SPs of index one, and with two other branches the two minima with index 0.

The situation changes further in panel B of Fig.5 where we obtain a real shoulder point. We insert the pseudo-convexity index (6)  $\mu = 0$  by black lines. Here the former



415  
416  
417  
418  
419  
420  
421  
422  
423  
424  
425  
426  
427  
428  
429  
430  
431  
432  
433  
434  
435  
436  
437  
438  
439  
440  
441  
442  
443  
444  
445  
446  
447  
448  
449  
450  
451  
452  
453  
454  
455  
456  
457  
458  
459  
460

**Fig. 5 A:** PES (8) for  $c=1.125$ . The former low SP and the former minimum  $M_2$  nearly merge and almost form a flat shoulder. The minimum  $M_1$  is still at the bottom, and the central SP also remains. **B:** PES for  $c=1.11$  which forms a PES with a shoulder point. Red is the rest of the singular NT through the VRI point, black dashed are GE curves, the pseudo-convexity index  $\mu = 0$  are black lines, and green are the IB lines.

$SP_{low}$  and the former minimum  $M_2$  have merged. The remaining point is a stationary point with a zero gradient and a zero eigenvector along the valley line. The PES is obtained by parameter  $c = 1.11$ . The shoulder is demonstrated by the GEs there, which do not cross as in stationary points but avoid a crossing near the former  $SP_{low}$ . Quasi three branches of the singular NT remain from the VRI. It is the limiting case. The next step is then the case of Fig.4 with  $c=1$ , where the character of the singular NT is lost, and where the connection to the former shoulder region also is finally lost.

Fig.6A shows an enlargement of the VRI region from Fig.5B. The black lines are the boundary of the pseudo-convexity (6)  $\mu = 0$ . In addition to the standard VRI point with a singular NT in red color through the dot symbol, a VB point also appears, at the cross,  $\times$ , where again the gradient is orthogonal to the GE direction. In contrast, at the plus  $+$  symbol, we find a crossing of GE and IB line with no orthogonal gradient direction to the GE. The point  $\times$  is crossed by an ordinary NT in brown color. In contrast, three special curves meet at the  $+$  symbol: a GE, an IB, and the  $\mu = 0$ -line. Here we have a loop of the singular NT, the former quasi-parallel branches to the shoulder. The point  $+$ , inside the loop, is the centre of a family of compact NTs, called centre NTs [38, 70]. One of these NTs is drawn in magenta color. NTs without stationary points are possible [68, 70]. We assume that they are not of deeper interest for chemical reasons. The VRIs are the most important definition, the first level in a hierarchy of valley bifurcations, so to speak. The VB of species  $\times$  forms the second level, which we should use if no VRI is there.

For comparison, we include still two neighboring NTs to the singular one, in Fig.6B, in blue color. The dashed NT follows the search direction  $(-1, 0.36)$ , it bypasses the VRI region on the right. The pure blue NT follows the  $(-1, 0.3)$  direction and runs to the SP at the left hand side of the VRI.

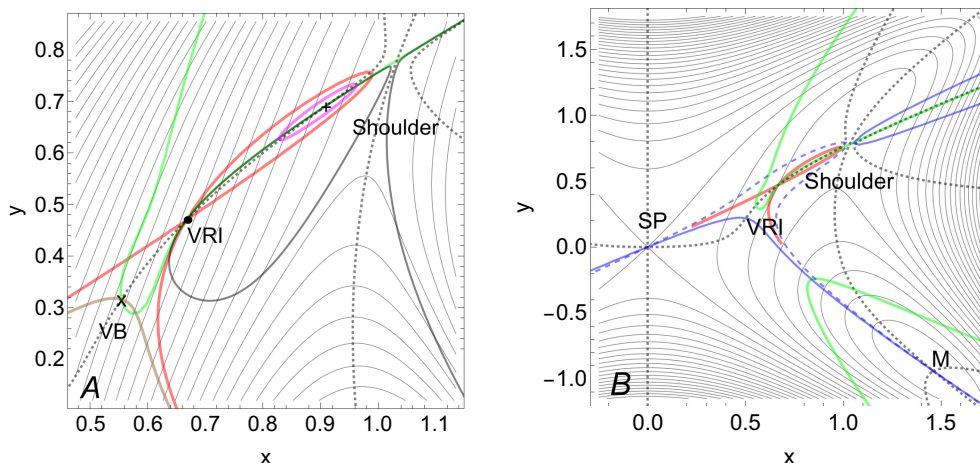


**Fig. 6** A: Enlargement of Fig.5B with a VB point,  $x$ , and a VRI point,  $\bullet$ , see text. B: Two regular NTs in blue are additionally included in Fig.5 B, see text.

Note that there is a parameter  $c$  nearby at  $\approx 1.10697$  where the VRI point and the point at the  $+$  symbol merge. Such a special singularity is called a cusp type [70]. For smaller values of  $c$  the VB point lefts over only.

## 4 Discussion

An important model for a reaction coordinate in chemistry is the steepest descent from SP, the intrinsic reaction coordinate (IRC) [29, 30]. In case of a symmetric PES and a totally symmetric axis through the SP [71–73], the IRC can cross a possible VRI point on this downhill path [31, 74–76]. However, on an asymmetric PES, the VRI is usually not located on the steepest descent from the SP [9, 77, 78]. There, any other reaction trajectory could bifurcate off from the IRC [79]. It is incorrect that the IRC splits itself at the VRI point [80, 81]. The IRC can split only at stationary points, where the gradient is zero, and where different directions for the further travel downhill can open. SPs are the singular points of the steepest descent trajectories. Analogous to NTs near VRI points, these trajectories follow hyperbolic curves around SPs.

One way out is a dynamical approach by many trajectories over the entrance SP region [19, 82–89]. This method contrasts with static models of a reaction pathway for IRC, NT, or GE. Localization through two sets of dynamical trajectories bifurcating near the VRI point is one way of a certain determination of the VRI point and product selectivity. Although dynamic trajectories can theoretically identify the VRI, this approach is unrealistic and hardly feasible in a real system. According to the ergodic hypothesis [90], a single trajectory could explore the entire configuration space if it moves forever in phase space, including the VRI. However, this is a multidimensional problem, and the growth of dimensions is proportional to the number of atoms involved. Finding a specific outcome amidst such complexity is highly unrealistic.

461  
462  
463  
464  
465  
466  
467  
468  
469  
470  
471  
472  
473  
474  
475  
476  
477  
478  
479  
480  
481  
482  
483  
484  
485  
486  
487  
488  
489  
490  
491  
492  
493  
494  
495  
496  
497  
498  
499  
500  
501  
502  
503  
504  
505  
506

507 The other possibility is the calculation of GEs and a singular NT to precisely  
 508 locate the VRI. Of course, this exceptional VB point of case  $c = 1$  of Fig.4 cannot be  
 509 detected using dynamical trajectories or a singular NT.

510 One can speculate that such VB points also exist on other, older known PES.  
 511 Because 'dead' valleys often exist. For example the well known Müller-Brown PES  
 512 [91] has such a valley on the left hand side, and no singular NT crosses it [68, 69].  
 513 In contrast, here also crosses a GE the IB line at point  $(x, y)=(-1.09771, 0.6487)$  and  
 514 the gradient is also nearly orthogonal to the GE direction, compare Fig. 7. This point  
 515 we propose for a VB indicator. The most left GE of the left valley ground intersects  
 516 also the IB line. There the gradient points in direction of the valley ground, which also  
 517 the GE follows. For the VB point it is more appropriate to use the GE being more  
 518 between the two bifurcating valleys.

519

520

521

522

523

524

525

526

527

528

529

530

531

532

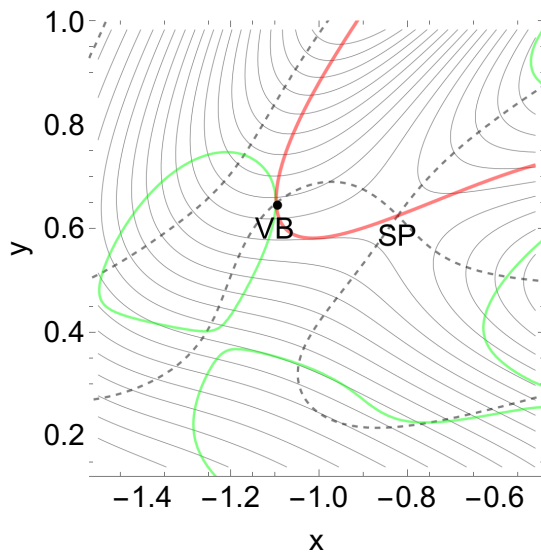
533

534

535

536

537



538

**Fig. 7** MB surface with proposed VB at the branching of the left global valley. Red is a regular NT, green are the IB lines.

539

540

541

542

## 5 Conclusion

543

544

545

546

547

548

549

550

551

552

We use Newton trajectories (NT), gradient extremals (GE) and lines of the boundaries of the Hessian index (IB) with  $\text{Det}(\mathbf{H})=0$  to explore the region of a VRI or a VB point. Long known are VRI points where a singular NT bifurcates. Its side branches form static models of a reaction path bifurcation. They can serve for models of trajectories to two different products.

By changing the parameter  $c$  of the PES of Ref. [33] we obtain a VB region with the special case of no singular NT. In the special situation of the VB point of this PES (8) with parameter  $c=1$ , the usual criteria for a VRI point, Eqs. (4) for NTs and (6) for GEs do not work appropriately. In contrast, a GE only crosses an IB line and

the gradient is orthogonal to the GE direction. This point we can accentuate for a VB point. One eigenvalue of the Hessian is zero, and the corresponding eigenvector is the gradient. Thus it holds Eq. (10). The nature of the PES of this case is that the one bifurcating valley is a ‘dead’ valley with no further stationary points. A ‘dead’ valley may be uninteresting for a chemical reaction, but it can be the basis for a vibration mode. The branching takes place without a ridge forming between the two new valleys. The ‘next ridge’ is the ridge that crosses the SP of the new side valley.

VRI and VB points form a hierarchy. The usual VRI points have been known for a long time. The VB points form a weaker level, which we should assign if a usual VRI is missing.

## Appendix 1: Proof of the Index Theorem

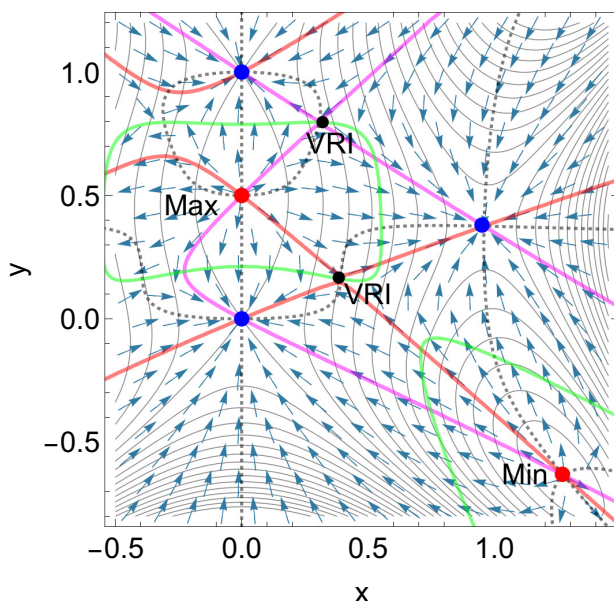


**Fig. 8** PES (8) with  $c=2$  now with an SP of index two, a maximum. Red points are stationary points with even indices, the minimum and the maximum, while blue points are three SPs of index one, three TSs. Two singular NTs cross two VRI points (black), one NT is red colored, and one NT is in magenta.

We follow references [68, 92, 93]. The Branin Eq. (2) is the desingularized continuous Newton equation. For the minus sign, it converges to a stationary point with an even index, i.e., a minimum with index zero as in the Newton-Raphson method. For plus sign, however, it converges to a stationary point with an odd index, compare Figs.2 and 4B. It can be developed with a Taylor approach for the gradient

$$\mathbf{g}(\mathbf{x}) \approx \mathbf{g}(\mathbf{x}_0) + \frac{\partial \mathbf{g}}{\partial \mathbf{x}}(\mathbf{x}_0) (\mathbf{x} - \mathbf{x}_0)$$

599 and for zero gradient at  $\mathbf{x}_0$  it is

600

601

$$= \mathbf{H}(\mathbf{x}_0) (\mathbf{x} - \mathbf{x}_0) .$$

602

603 Eq.(2) looks then

604

605

$$\frac{d\mathbf{x}}{dt} \approx -\mathbf{A}(\mathbf{x})\mathbf{H}(\mathbf{x}_0) (\mathbf{x} - \mathbf{x}_0) \approx -\text{Det}(\mathbf{H}(\mathbf{x}_0)) (\mathbf{x} - \mathbf{x}_0) ,$$

606

607

608 and this is attractive for even index, but repulsive for odd index of  $\mathbf{H}(\mathbf{x}_0)$ .

609

610 For illustration, Fig.8 shows a test surface with three types of stationary points.

611

612 Regular NTs from the maximum at  $(0,0.5)$  only lead to SPs of index one, and so

613

614 on. Thus starting near of one of the two kinds of stationary points, an NT (with

615

616 corresponding  $\pm$  change) will lead to the other kind, by an index difference of one.

617

618 This rule can only be violated by a VRI point on a singular NT.

619

620

621

622

623

624

625

626

627

628

629

630

631

632

633

634

635

636

637

638

639

640

641

642

643

644

## Appendix 2: Discussion of GE bifurcations

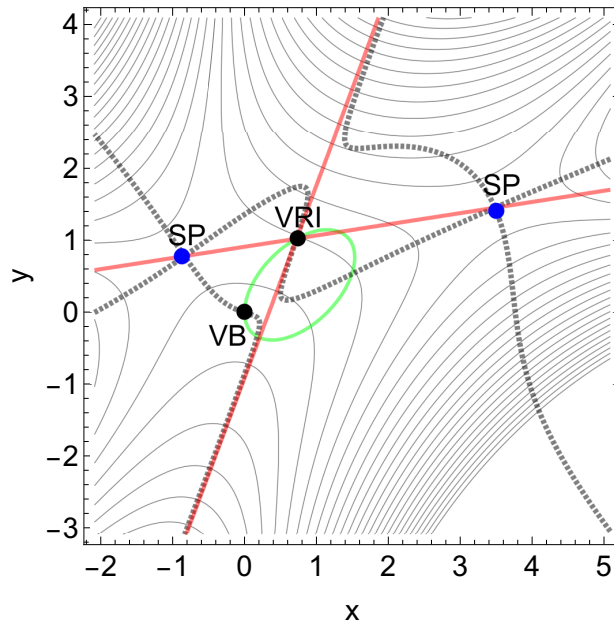


Fig. 9 PES with avoided crossings of GEs (black dashes). Blue points are SPs. Two branches of the singular NT (red) cross at the VRI point a GE. An additional VB point is included, see text.

On a symmetric PES, a valley GE can bifurcate and indicate the branching of the PES [67]. Which criterion we apply may depend on the problem to be solved.

Now we study the avoided crossing of GEs, which is the usual behavior of GEs on an asymmetric PES, see Fig. 9. An artificial 2D PES [63] is

$$V(x, y) = x y (y - x) + 1.15 x^2 + 2 y - 3 .$$

Dotted curves represent three GEs, the two red lines are the singular NT and the green elliptic curve is the IB line. In the center is the intersection of the GE from left to right and the red singular NT. It is a common VRI point. The GEs themselves only cross at the SPs. The aim of recognising a VB by the crossing of the GEs would therefore fail here.

However, a valley bifurcation before the VRI can be assumed, below the level of the SPs, which is indicated by an additional VB point shown. It is the intersection of the left GE with the IB line where the gradient is orthogonal to the GE.

### Appendix 3: Representation of NTs and of GEs

#### 2D PES with NTs [68]

In 2D toy examples, NTs can easily be represented by a graphical rule. It applies in two dimensions that the orthogonal direction to the force direction

$$\mathbf{f} = \begin{pmatrix} f_1 \\ f_2 \end{pmatrix} \text{ is unique the direction } \mathbf{f}^\perp = (-f_2, f_1) .$$

Then condition (1) that  $\mathbf{f} \parallel \mathbf{g}$  is the zero of the scalar product

$$\mathbf{f}^\perp \cdot \mathbf{g} = 0 .$$

In Mathematica, one can represent the corresponding NT by  
`ContourPlot[-g1[x,y] f2[x,y] + g2[x,y] f1[x,y],{x,-2,2},{y,-2,2}, ContourShading->False, Contours->{0.0}]`

#### 2D PES with GEs

In analogy to NTs, also GEs can easily be represented by a graphical rule in 2D examples. It applies in two dimensions that the orthogonal direction to the gradient direction

$$\mathbf{g} = \begin{pmatrix} g_1 \\ g_2 \end{pmatrix} \text{ is unique the direction } \mathbf{g}^\perp = (-g_2, g_1) .$$

Then condition (5) means that  $\mathbf{H} \mathbf{g} \parallel \mathbf{g}$ , and this is again the zero of the scalar product

$$\mathbf{g}^\perp \cdot \mathbf{H} \mathbf{g} = 0 .$$

One can display the corresponding GE in a graphic program analogously to above.

691 **Conflict of Interest:** We declare that we have no affiliation with or involvement in any  
692 organization that has a financial interest in the subject matter or materials discussed herein.

693  
694 **Author Contributions:** WQ, HHGCh and JMB contributed equally.

695  
696 **Methods:** We have used Mathematica 13.3.1.0 for Linux x86(64-bit) in the calculations and  
697 in the representation of the figures.

698  
699 **Data Access Statement:** All relevant data are included in the paper. Further data can be  
700 obtained from WQ.

701  
702 **Acknowledgements:**

703 We thank a reviewer for suggesting Fig.6A, Fig.9, and for many questions and important  
704 comments.

705 JMB thanks the Spanish Structures of Excellence María de Maeztu Program, Grant  
706 CEX2021-001202-M, and the Agència de Gestió d’Ajuts Universitaris i de Recerca of Gener-  
707 alitat de Catalunya, Projecte 2021 SGR 00354.

708 GHHCh acknowledges support from the Max-Planck Gesellschaft via the MPI-PKS visitors  
709 program.

## 710 **References**

711 [1] Stewart, I.: Applications of catastrophe theory to the physical sciences. *Physica*  
712 *D* **2**, 245–305 (1981)

713  
714 [2] Crawford, J.D.: Introduction to bifurcation theory. *Rev. Mod. Phys.* **63**, 991–1037  
715 (1991)

716  
717 [3] Valtazanos, P., Ruedenberg, K.: Bifurcations and transition states. *Theor. Chim.*  
718 *Acta* **69**, 281–307 (1986)

719  
720 [4] Baker, J., Gill, P.M.W.: An algorithm for the location of branching points on  
721 reaction paths. *J. Comput. Chem.* **9**, 465–475 (1988)

722  
723 [5] Yamamoto, N., Bernardi, F., Bottoni, A., Olivucci, M., Robb, M.A., Wilsey,  
724 S.: Mechanism of carbene formation from the excited states of diazirine and  
725 diazomethane: An MC-SCF study. *J. Am. Chem. Soc.* **116**, 2064–2074 (1994)

726  
727 [6] Quapp, W., Hirsch, M., Heidrich, D.: Bifurcation of reaction pathways: the set  
728 of valley ridge inflection points of a simple three-dimensional potential energy  
729 surface. *Theor. Chem. Acc.* **100**(5/6), 285–299 (1998)

730  
731 [7] Margalef-Roig, J., Miret-Artes, S., Toro-Labbe, A.: Characterization of ele-  
732 mentary chemical reactions from bifurcation theory. *J. Phys. Chem. A* **104**,  
733 11589–11592 (2000)

734  
735 [8] Quapp, W., Hirsch, M., Heidrich, D.: An approach to reaction path branching  
736 using valley-ridge inflection points of potential energy surfaces. *Theor. Chem.*



Acc. <b>112</b> , 40–51 (2004)	737
	738
[9] Suhrada, C.P., Selcuki, S., Nendel, N., Cannizzaro, C., Houk, K.N., Rissing, P.-J., Baumann, D., Hasselmann, D.: Dynamic effects on [3,3] and [1,3] shifts of 6- methylenebicyclo[3.2.0]hept-2-ene. <i>Angew. Chem., Int. Ed.</i> <b>44</b> , 3548–3552 (2005)	739 740 741
	742
[10] Goldsmith, B.R., Sanderson, E.D., Bean, D., Peters, B.: Isolated catalyst sites on amorphous supports: A systematic algorithm for understanding heterogeneities in structure and reactivity. <i>J. Chem. Phys.</i> <b>138</b> , 204105 (2013)	743 744 745
	746
[11] Windhorn, L., Yeston, J.S., Witte, T., Fuss, W., Motzkus, M., Proch, D., Kompa, K.L., Moore, C.B.: Getting ahead of IVR: A demonstration of mid-infrared induced molecular dissociation on a sub-statistical time scale. <i>J. Chem. Phys.</i> <b>119</b> , 641–644 (2003)	747 748 749 750
	751
[12] Michel, L.: Symmetry defects and broken symmetry. Configurations. Hidden symmetry. <i>Rev. Mod. Phys.</i> <b>52</b> , 617–651 (1980)	752 753
	754
[13] Kraus, W.A., DePristo, A.E.: Reaction dynamics on bifurcating potential energy surfaces. <i>Theoret. Chim. Acta</i> <b>69</b> , 309–322 (1986)	755 756
	757
[14] Bakken, V., Danovich, D., Shaik, S., Schlegel, H.B.: A single transition state serves two mechanisms: An ab initio classical trajectory study of the electron transfer and substitution mechanisms in reactions of ketyl radical anions with alkyl halides. <i>J. Am. Chem. Soc.</i> <b>123</b> , 130–134 (2001)	758 759 760
	761
[15] Limanto, J., Khuong, K.S., Houk, K.N., Snapper, M.L.: Intramolecular cycload- ditions of Cyclobutadiene with Dienes: Experimental and computational studies of the competing (2 + 2) and (4 + 2) modes of reaction. <i>J. Am. Chem. Soc.</i> <b>125</b> , 16310–16321 (2003)	762 763 764 765
	766
[16] Lasorne, B., Dive, G., Lauvergnat, D., Desouter-Lecomte, M.: Wave packet dynamics along bifurcating reaction paths. <i>J. Chem. Phys.</i> <b>118</b> (13), 5831–5840 (2003)	767 768 769
	770
[17] Zheng, J., Papajak, E., Truhlar, D.G.: Phase space prediction of product branch- ing ratios: Canonical competitive nonstatistical model. <i>J. Am. Chem. Soc.</i> <b>131</b> (43), 15754–15760 (2009)	771 772 773
	774
[18] Rehbein, J., Carpenter, B.K.: Do we fully understand what controls chemical selectivity? <i>Phys. Chem. Chem. Phys.</i> <b>13</b> , 20906–20922 (2011)	775 776
	777
[19] Ohashi, M., Liu, F., Hai, Y., Chen, M., Tang, M.-c., Yang, Z., Sato, M., Watanabe, K., Houk, K.N., Tang, Y.: SAM-dependent enzyme-catalysed pericyclic reactions in natural product biosynthesis. <i>Nature</i> <b>549</b> , 502–506 (2017)	778 779 780
	781
[20] Ge, L., Li, S., George, T.F., Sun, X.: A model of intrinsic symmetry breaking.	782

- 783 Phys. Lett. A **377**, 2069–2073 (2013)  
784
- 785 [21] Sanchez-Galvez, A., Hunt, P., Robb, M.A., Olivucci, M., Vreven, T., Schlegel,  
786 H.B.: Ultrafast radiationless deactivation of organic dyes: evidence for a two-state  
787 two-mode pathway in polymethine cyanines. *J. A. Chem. Soc.* **122**, 2911–2924  
788 (2000)
- 789 [22] Wang, Z., Hirschi, J.S., Singleton, D.A.: Recrossing and dynamic matching effects  
790 on selectivity in a Diels-Alder reaction. *Angew. Chem. Int. Ed Engl.* **48**(48),  
791 9156–9159 (2009)  
792
- 793 [23] Chuang, H.-H., Tantillo, D.J., Hsu, C.-P.: Construction of two-dimensional poten-  
794 tial energy surfaces of reactions with post-transition-state bifurcations. *J. Chem.*  
795 *Theory Computat.* **16**(7), 4050–4060 (2020)  
796
- 797 [24] Çelebi-Ölçüm, N., Ess, D.H., Aviyente, V., Houk, K.N.: Lewis acid catalysis alters  
798 the shapes and products of bis-pericyclic Diels-Alder transition states. *J. Am.*  
799 *Chem. Soc.* **129**, 4528–4529 (2007)  
800
- 801 [25] Ess, D.H., Wheeler, S.E., Iafe, R.G., Xu, L., Çelebi-Ölçüm, N., Houk, K.N.: Bifur-  
802 cations on potential energy surfaces of organic reactions. *Angew. Chem. Int. Ed.*  
803 **47**, 7592–7601 (2008)  
804
- 805 [26] Lee, S., Goodman, J.M.: Rapid route-finding for bifurcating organic reactions. *J.*  
806 *Am. Chem. Soc.* **142**(20), 9210–9219 (2020)  
807
- 808 [27] Katsanikas, M., Garcia-Garrido, V.J., Agaoglou, M., Wiggins, S.: Phase space  
809 analysis of the dynamics on a potential energy surface with an entrance channel  
810 and two potential wells. *Phys. Rev. E* **102**, 012215 (2020)  
811
- 812 [28] Crossley, R., Agaoglou, M., Katsanikas, M., Wiggins, S.: From Poincaré maps  
813 to Lagrangian descriptors: The case of the valley ridge inflection point potential.  
814 *Regul. Chaot. Dyn.* **26**, 147–164 (2021)
- 815 [29] Fukui, K.: A formulation of the reaction coordinate. *J. Phys. Chem.* **74**, 4161–4163  
816 (1970)  
817
- 818 [30] Quapp, W., Heidrich, D.: Analysis of the concept of minimum energy path on the  
819 potential energy surface of chemically reacting systems. *Theor. Chim. Acta* **66**,  
820 245–260 (1984)  
821
- 822 [31] Taketsugu, T., Yanai, T., Hirao, K., Gordon, M.S.: Dynamic reaction path study  
823 of  $\text{SiH}_4 + \text{F}^- \rightarrow \text{SiH}_4\text{F}^-$  and the Berry pseudorotation with valley-ridge inflection.  
824 *J. Molec. Struc.: THEOCHEM* **451**(1-2), 163–177 (1998)  
825
- 826 [32] Maeda, S., Harabuchi, Y., Ono, Y., Taketsugu, T., Morokuma, K.: Intrinsic reac-  
827 tion coordinate: Calculation, bifurcation, and automated search. *Int. J. Quant.*  
828

Chem. <b>115</b> , 258–269 (2015)	829
	830
[33] Su, H., Wang, H., Zhang, L., Zhao, J., Zheng, X.: Improved high-index saddle dynamics for finding saddle points and solution landscape. arXiv <b>2502.03694v2</b> , 1–19 (2025)	831
	832
	833
	834
[34] Quapp, W., Bofill, J.M.: A contribution to a theory of mechanochemical pathways by means of Newton trajectories. <i>Theoret. Chem. Acc.</i> <b>135</b> (4), 113 (2016)	835
	836
	837
[35] Quapp, W., Bofill, J.M., Ribas-Arino, J.: Towards a theory of mechanochemistry-simple models from the very beginning. <i>Int. J. Quant. Chem.</i> <b>118</b> , 25775 (2018)	838
	839
[36] Quapp, W., Bofill, J.M.: Theory and examples of catch bonds. <i>J. Phys. Chem. B</i> <b>128</b> (17), 4097–4110 (2024)	840
	841
	842
[37] Branin, F.H.: Widely convergent methods for finding multiple solutions of simultaneous nonlinear equations. <i>IBM J. Res. Develop.</i> <b>16</b> , 504–522 (1972)	843
	844
	845
[38] Jongen, H.T., Jonker, P., Twilt, F.: <i>Nonlinear Optimization in Finite Dimensions</i> . Kluwer Academic Publ., Dordrecht (2000)	846
	847
	848
[39] Bofill, J.M.: Updated Hessian matrix and the restricted step method for locating transition structures. <i>J. Computat. Chem.</i> <b>15</b> , 1–11 (1994)	849
	850
	851
[40] Anglada, J.M., Besalú, E., Bofill, J.M., Rubio, J.: Another way to implement the Powell formula for updating Hessian matrices related to transition structures. <i>J. Math. Chem.</i> <b>25</b> , 85–92 (1999)	852
	853
	854
	855
[41] Hratchian, H.P., Schlegel, H.B.: Using Hessian updating to increase the efficiency of a Hessian based predictor-corrector relation path following method. <i>J. Chem. Theory Computat.</i> <b>1</b> , 61 (2005)	856
	857
	858
[42] Bofill, J.M., Quapp, W.: Variational nature, integration, and properties of the Newton reaction path. <i>J. Chem. Phys.</i> <b>134</b> , 074101 (2011)	859
	860
	861
[43] Hirsch, M., Quapp, W., Heidrich, D.: The set of valley-ridge inflection points on the potential energy surface of the water molecule. <i>Phys. Chem. Chem. Phys.</i> <b>1</b> , 5291–5299 (1999)	862
	863
	864
	865
[44] Quapp, W., Melnikov, V.: The set of valley ridge inflection points on the potential energy surfaces of H <sub>2</sub> S, H <sub>2</sub> Se and H <sub>2</sub> CO. <i>Phys. Chem. Chem. Phys.</i> <b>3</b> , 2735–2741 (2001)	866
	867
	868
	869
[45] Bofill, J.M., Quapp, W.: Analysis of the valley-ridge inflection points through the partitioning technique of the Hessian eigenvalue equation. <i>J. Math. Chem.</i> <b>51</b> , 1099–1115 (2013)	870
	871
	872
	873
[46] Quapp, W., Bofill, J.M., Aguilar-Mogas, A.: Exploration of cyclopropyl radical	874

875 ring opening to allyl radical by Newton trajectories: Importance of valley-ridge  
876 inflection points to understand the topography. *Theor. Chem. Acc.* **129**, 803–821  
877 (2011)  
878  
879 [47] Quapp, W.: Can we understand the branching of reaction valleys for more than  
880 two degrees of freedom? *J. Math. Chem.* **54**, 137–148 (2015)  
881  
882 [48] COLUMBUS: program system. [https://columbus-program-system.gitlab.io/  
883 columbus/](https://columbus-program-system.gitlab.io/columbus/) (2023)  
884  
885 [49] Quapp, W.: Program for unsymmetric valley-ridge inflection points.  
886 [www.math.uni-leipzig.de/~quapp/SkewVRIs.html](http://www.math.uni-leipzig.de/~quapp/SkewVRIs.html) (2011)  
887  
888 [50] Quapp, W.: Mathematica notebook for catch bond calculations.  
889 <https://community.wolfram.com/groups/-/m/t/3167380> , **Wolfram** (2024)  
890  
891 [51] Quapp, W., Schmidt, B.: An empirical, variational method of approach to  
892 unsymmetric valley-ridge inflection points. *Theor. Chem. Acc.* **128**, 47–61 (2011)  
893  
894 [52] Schmidt, B., Quapp, W.: Search of manifolds of nonsymmetric valley-ridge inflec-  
895 tion points on the potential energy surface of HCN. *Theor. Chem. Acc.* **132**,  
896 1305–1313 (2012)  
897  
898 [53] Garcia-Garrido, V.J., Wiggins, S.: The dynamical significance of valley-ridge  
899 inflection points. *Chem. Phys. Lett.* **781**, 138970 (2021)  
900  
901 [54] Gonzalez, J., Gimenez, X., Bofill, J.M.: A reaction path Hamiltonian defined on  
902 a Newton path. *J. Chem. Phys.* **116**, 8713–8722 (2002)  
903  
904 [55] Quapp, W.: A growing string method for the reaction pathway defined by a  
905 Newton trajectory. *J. Chem. Phys.* **122**, 174106 (2005)  
906  
907 [56] Konda, S.S.M., Brantley, J.M., Bielawski, C.W., Makarov, D.E.: Chemical reac-  
908 tions modulated by mechanical stress: Extended Bell theory. *J. Chem. Phys.* **135**,  
909 164103 (2011)  
910  
911 [57] Cardozo, T.M., Galliez, A.P., Borges Jr, I., Plasser, F., Aquino, A.J.A., Bar-  
912 batti, M., Lischka, H.: Dynamics of benzene excimer formation from the  
913 parallel-displaced dimer. *Phys. Chem. Chem. Phys.* **21**, 13916–13924 (2019)  
914  
915 [58] Barkan, C.O., Bruinsma, R.F.: Topology of molecular deformations induces  
916 triphasic catch bonding in selectin-ligand bonds. *Proc. Natl. Acad. Sci.* **121**,  
917 2315866121 (2024)  
918  
919 [59] Hopper, N., Rana, R., Sidoroff, F., Cayer-Barrioz, J., Mazuyer, D., Tysoe, W.T.:  
920 Activation volumes in tribochemistry; what do they mean and how to calculate  
them? *Tribol. Lett.* **73**, 40 (2025)

[60]	Quapp, W.: Finding the transition state without initial guess: the growing string method for Newton trajectory to isomerisation and enantiomerisation reaction of alanine dipeptide and poly(15)alanine. <i>J. Computat. Chem</i> <b>28</b> , 1834–1847 (2007)	921 922 923 924
[61]	Hoffmann, D.K., Nord, R.S., Ruedenberg, K.: Gradient extremals. <i>Theor. Chim. Acta</i> <b>69</b> , 265–280 (1986)	925 926 927
[62]	Sun, J.-Q., Ruedenberg, K.: Gradient extremals and steepest descent lines on potential energy surfaces. <i>J. Chem. Phys.</i> <b>98</b> , 9707–9714 (1993)	928 929 930
[63]	Quapp, W.: Gradient Extremals and Valley Floor Bifurcation on Potential Energy Surfaces. <i>Theoret. Chim. Acta</i> <b>75</b> , 447–460 (1989)	931 932 933
[64]	Schlegel, H.B.: Following gradient extremal paths. <i>Theor. Chim. Acta</i> <b>83</b> , 15–20 (1992)	934 935 936
[65]	Hirsch, M., Quapp, W.: Reaction pathways and convexity of the potential energy surface: Application of Newton trajectories. <i>J. Math. Chem.</i> <b>36</b> , 307–340 (2004)	937 938 939
[66]	Bofill, J.M., Quapp, W., Caballero, M.: The variational structure of gradient extremals. <i>J. Chem. Theory Computat.</i> <b>8</b> , 927–935 (2012)	940 941 942
[67]	Quapp, W., Hirsch, M., Heidrich, D.: Following the streambed reaction on potential energy surfaces: a new robust method. <i>Theor. Chem. Acc.</i> <b>105</b> , 145–155 (2000)	943 944 945
[68]	Hirsch, M.: Zum Reaktionswegcharakter von Newtontrajektorien (in german). Dissertation, University Leipzig, Faculty of Chemistry and Mineralogy (2004)	946 947 948
[69]	Quapp, W., Bofill, J.M.: Mechanochemistry on the Müller-Brown surface by Newton trajectories. <i>Int. J. Quant. Chem.</i> <b>118</b> , 25522 (2018)	949 950 951
[70]	Hirsch, M., Quapp, W.: Reaction Channels of the Potential Energy Surface: Application of Newton Trajectories. <i>J. Molec. Struct., THEOCHEM</i> <b>683</b> (1-3), 1–13 (2004)	952 953 954
[71]	Pechukas, P.: On simple saddle points of a potential surface, the conservation of nuclear symmetry along paths of steepest descent, and the symmetry of transition states. <i>J. Chem. Phys.</i> <b>64</b> , 1516–1521 (1976)	955 956 957 958
[72]	Bone, R.G.A.: Deducing the symmetry operations generated at the transition state. <i>Chem. Phys. Lett.</i> <b>193</b> , 557–564 (1992)	959 960 961
[73]	Schaad, L.J., Hu, J.: Symmetry rules for transition structures in degenerate reactions. <i>J. Am. Chem. Soc.</i> <b>120</b> , 1571–1580 (1998)	962 963 964
[74]	Minyaev, R.M., Wales, D.J.: Gradient line reaction path of HF addition to ethylene. <i>Chem. Phys. Lett.</i> <b>218</b> (5-6), 413–421 (1994)	965 966

- 967 [75] Harabuchi, Y., Taketsugu, T.: A significant role of the totally-symmetric valley-  
968 ridge inflection point in the bifurcating reaction pathway. *Theoret. Chem. Acc.*  
969 **130**, 305–315 (2011)  
970
- 971 [76] Zhou, C., Birney, D.M.: Sequential transition states and the valley-ridge inflection  
972 point in the formation of a semibullvalene. *Organic Lett.* **4**, 3279–3282 (2002)  
973
- 974 [77] Debbert, S.L., Carpenter, B.K., Hrovat, D.A., Borden, W.T.: The iconoclastic  
975 dynamics of the 1,2,6-heptatriene rearrangement. *J. Am. Chem. Soc.* **124**, 7896–  
976 7897 (2002)
- 977 [78] Pomerantz, A., Camden, J.P., Chioiu, A.S., Ausfelder, F., Chawia, N., Hase,  
978 W.L., Zare, R.N.: Reaction products with internal energy beyond the kinematic  
979 limit result from trajectories far from the minimum energy path: An example  
980 from  $\text{H} + \text{HBr} \rightarrow \text{H}_2 + \text{Br}$ . *J. Am. Chem. Soc.* **127**(47), 16368–16369 (2005)  
981
- 982 [79] Okada, K., Sugimoto, M., Saito, K.: A reaction-path dynamics approach to the  
983 thermal unimolecular decomposition of acetaldoxime. *Chem. Phys.* **189**, 629–636  
984 (1994)  
985
- 986 [80] Shustov, G.V., Rauk, A.: Mechanism of dioxirane oxidation of CH bonds, appli-  
987 cation to homo- and heterosubstituted alkanes as a model of the oxidation of  
988 peptides. *J. Organic Chem.* **63**(16), 5413–5422 (1998)  
989
- 990 [81] Carpenter, B.K., Harvey, J., Glowacki, D.: Prediction of enhanced solvent-induced  
991 enantioselectivity for a ring opening with a bifurcating reaction path. *Phys. Chem.*  
992 *Chem. Phys.* **17**, 8372–8381 (2015)  
993
- 994 [82] Mann, D.J., Hase, W.L.: Ab initio direct dynamics study of cyclopropyl radical  
995 ring-opening. *J. Am. Chem. Soc.* **124**, 3208–3209 (2002)  
996
- 997 [83] Taketsugu, T., Kumeda, Y.: An ab initio direct-trajectory study of the kinetic  
998 isotope effect on the bifurcating reaction. *J. Chem. Phys.* **114**, 6973–6982 (2001)  
999
- 1000 [84] Gonzalez-Lafont, A., Moreno, M., Lluch, J.M.: Variational transition state theory  
1001 as a tool to determine kinetic selectivity in reactions involving a valley-ridge  
1002 inflection point. *J. Am. Chem. Soc.* **126**, 13089–13094 (2004)
- 1003 [85] Ussing, B.R., Hang, C., Singleton, D.A.: Dynamic effects on the periselectivity,  
1004 rate, isotope effects, and mechanism of cycloadditions of ketenes with  
1005 cyclopentadiene. *J. Am. Chem. Soc.* **128**, 7594–7607 (2006)  
1006
- 1007 [86] Thomas, J.B., Waas, J.R., Harmata, M., Singleton, D.A.: Control elements in  
1008 dynamically determined selectivity on a bifurcating surface. *J. Am. Chem. Soc.*  
1009 **130**, 14544–14555 (2008)  
1010
- 1011 [87] Yamamoto, Y., Hasegawa, H., Yamataka, H.: Dynamic path bifurcation in the  
1012

Beckmann reaction: Support from kinetic analyses. <i>J. Org. Chem.</i> <b>76</b> , 4652–4660 (2011)	1013 1014 1015
[88] Hong, Y.J., Tantillo, D.J.: Biosynthetic consequences of multiple sequential post-transition-state bifurcations. <i>Nat. Chem.</i> <b>6</b> , 104–111 (2014)	1016 1017 1018
[89] Kong, W.-Y., Hu, Y., Guo, W., Potluri, A., Schomaker, J.M., Tantillo, D.J.: Synthetically relevant post-transition state bifurcation leading to diradical and zwitterionic intermediates: Controlling nonstatistical kinetic selectivity through solvent effects. <i>J. Am. Chem. Soc.</i> (2025)	1019 1020 1021 1022 1023
[90] Boltzmann, L.: <i>Vorlesungen über Gastheorie</i> . J. A. Barth, Leipzig (1898)	1024 1025
[91] Müller, K., Brown, L.D.: Location of saddle points and minimum energy paths by a constrained simplex optimisation procedure. <i>Theor. Chim. Acta</i> <b>53</b> , 75–93 (1979)	1026 1027 1028
[92] Diener, I.: <i>Globale Aspekte des kontinuierlichen Newtonverfahrens</i> . Habilitation, University Göttingen, Göttingen (1991)	1029 1030 1031
[93] Diener, I.: Trajectory methods in global optimization. In: Horst, R., Pardalos, P.M. (eds.) <i>Handbook of Global Optimization. Nonconvex Optimization and Its Applications</i> , vol. 2, pp. 649–668. Springer, US (1995)	1032 1033 1034 1035 1036 1037 1038 1039 1040 1041 1042 1043 1044 1045 1046 1047 1048 1049 1050 1051 1052 1053 1054 1055 1056 1057 1058